Phase diagrams of random Ising magnets

M. F. Thorpe and A. R. McGurn

Physics Department, Michigan State University,
East Lansing, Michigan 48824
(Received 25 October 1978)

We examine the various kinds of phase diagrams that can occur in magnetic alloys when all the interactions have the same sign, i.e., all ferromagnetic. It is pointed out that these phase diagrams can be usefully cataloged in terms of the initial slope $[\partial(\ln T_c)/\partial p]$ of the transition temperature T_c with concentration p at the two points $p = 0$ and $p = 1$. For the two-dimensional Ising model, these initial slopes can be obtained exactly, using perturbation theory, for alloys involving either bond or site disorder. For site disorder we obtain results for a spin S in a host with spin $\frac{1}{2}$. We show that mean-field theory is fairly reliable but fails to predict some kinds of phase diagrams that may occur.

I. INTRODUCTION

Increasing interest has been shown recently in the phase diagrams of insulating magnetic alloys. A few of these systems have now been studied[1] and it is very probable that many more will be studied over the next few years. These systems (e.g., $RbMn_pNi_{1-p}F_3$, $K_2Mn_pCo_{1-p}F_4$, etc.[1]) are very attractive to study because the interactions are short ranged (often predominantly nearest neighbor) and so present a well-defined challenge to theory in explaining the behavior of the transition temperature T_c with concentration p. Of course there are many other properties of alloys such as the specific heat, susceptibility, and the critical exponents that one would like to explain. However these are more complicated questions and we will only discuss $T_c(p)$ in this paper. This can usually be obtained experimentally by searching for discontinuities in either the specific heat or in the susceptibility. This is not always easy due to rounding caused by inhomogeneities, etc.

There are a number of approximate methods for obtaining complete phase diagrams and we shall discuss some of these in this paper: mean-field theory, annealed models for alloys with bond disorder, and the Bethe lattice construction. No exact calculations of the phase diagram exist, with the exception of the very restricted form of the randomness in the two-dimensional Ising model of McCoy and Wu.[2]

In this paper we consider two kinds of disordered systems. Both are Ising ferromagnets with only nearest-neighbor exchange. For a ferromagnet with *bond disorder*, there are two kinds of bonds with strengths J_1 and J_2 that are positioned randomly throughout the system with probability p and $1-p$, respectively. For a ferromagnet with *site disorder*, there are two kinds of sites A and B that are positioned randomly throughout the system with probability p and $1-p$, respectively. As a consequence

there are three kinds of bonds with strengths J_{AA}, J_{BB}, and $J_{AB} = J_{BA}$.

The initial slope $\partial(\ln T_c)/\partial p$ for $p = 0$ and $p = 1$ can be calculated exactly using perturbation theory for Ising models where the disorder is of either the bond or site kind. The result is expressed in terms of correlation functions in the pure system which are known exactly in two dimensions. For the two-component systems that we are considering here, these initial slopes determine the *overall character of the phase diagram* although not the detailed shape of course. In Sec. II we introduce a general classification scheme based on the initial slopes.

The alloy with bond disorder is simpler to treat theoretically and we study this in Sec. III. This corresponds to having two ligands through which the superexchange can take place, leading to two possible exchange interactions between neighboring magnetic ions. This case has not been much studied experimentally [an exception is $Co(S_pSe_{1-p})_2$].[3] More experimental work on these systems would be helpful as they are the simplest of all alloy systems.

In Sec. IV we discuss site disorder. The perturbation theory is a little more complicated here, but proceeds in a very similar manner to that for bond disorder. We find a much richer variety of behavior because an extra parameter J_{AB}, the exchange between magnetic ions at A and B sites, is involved. We show that our conclusions about what kinds of behavior are possible are not very dependent on spin, by studying a site impurity with $S > \frac{1}{2}$.

Much of the detailed calculation is relegated to the Appendices so as not to interrupt the flow of the paper.

II. GENERAL CLASSIFICATION SCHEME

Perturbation theory leads to the initial slope $\partial(\ln T_c)/\partial p$ for $p = 0$ and $p = 1$, where p is the bond

(site) concentration for bond (site) disorder. Although this by no means provides a complete description of the phase diagram, it does severely restrict what can occur and so can be used as the basis of a classification scheme.

If there is no competition between the exchange interactions, i.e., they are all ferromagnetic, then we expect only two phases to occur—paramagnetic at high temperatures and ferromagnetic at low temperatures. This is borne out by all approximate calculations of the complete phase diagram.

Consider an alloy with a transition temperature $T_c(p)$ as a function of the concentration p. We can suppose without loss of generality that $T_c(1) > T_c(0)$. The simplest possible phase boundary would be a straight line extrapolation for $T_c(p)$ between $T_c(0)$ and $T_c(1)$ as shown in the upper part of Fig. 1 by a dashed line. From the *initial slopes near $p = 0$*, we can identify three possible types of behavior also in-
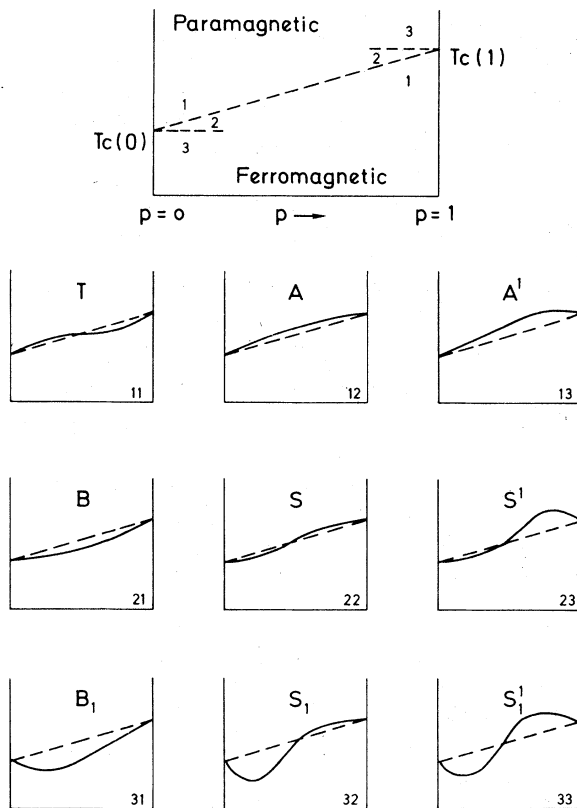

FIG. 1. Upper part of the figure shows the linear extrapolation of the phase boundary between $T_c(0)$ and $T_c(1)$ that divides the ordered from the disordered phase. The nine phase diagrams below are indexed according to the three possible behaviors of the initial slopes at either end of the phase diagrams (denoted by 1, 2, or 3). The labelling (A, B, S, T) is explained in the text and the superscripts and subscripts show if there is a maximum or minimum in the phase diagram.

dicated in the upper part of Fig. 1: (i) having slope greater than the linear extrapolation, (ii) having a slope less than the linear extrapolation but greater than zero, (iii) having a slope less than zero. There are three similar types of behavior near $p = 1$ giving a set of *nine phase diagrams* that are indexed by ij in the lower part of Fig. 1, where i refers to the behavior near $p = 0$ and j to the behavior near $p = 1$. Each of the nine phase diagrams is the *simplest possible* compatible with the initial slopes. It is possible that the phase boundaries could have many more maxima and minima and still be compatible with the initial slopes. For the simple two-component alloys that we study in this paper, this more complex behavior would be unlikely to occur and is not suggested by any experiment or approximate theory that we know of.

In order to give these possible sets of phase diagrams a labelling that is somewhat easier to remember than the ij labelling, we have adopted the following notation which emphasizes the behavior with respect to the dashed linear extrapolation and also the number of maxima and minima. In this notation we write X_m^n where m,n is the number of minima, maxima (never greater than 1 for the simplest possible phase diagrams shown in Fig. 1). If n or m is equal to zero, it is omitted. The letter X can be either A for above, B for below, S for straddle, or T for transverse. This designates the behavior with respect to the dashed line and T is the mirror image of S with respect to the dashed line. We note again that we have put $T_c(1) > T_c(0)$. If this were not so, then p could be redefined as $1-p$ and it would be so. Our simple classification scheme therefore exhausts all possibilities—assuming of course that $T_c(p)$ never drops to zero. This is the reason that we have restricted ourselves to cases where all the exchanges have the same sign (excluding zero) and where $k_B T_c(p) \gtrsim \min(J_{ij}) > 0$.

III. BOND DISORDER

Although bond disorder is not as readily accessible experimentally as site disorder [an exception is $Co(S_p Se_{1-p})_2$],[3] we will discuss it first as it is rather simpler to treat theoretically. The Hamiltonian for the system is

$$H = -4 \sum_{\langle ij \rangle} J_{ij} S_i^z S_j^z , \qquad (3.1)$$

where the probability distribution of exchange parameters J_{ij} is a product of terms for each bond; each with the same form

$$P(J_{ij}) = p\,\delta(J_{ij} - J_1) + (1-p)\,\delta(J_{ij} - J_2) . \qquad (3.2)$$

This is sometimes referred to as *quenched disorder*. The factor 4 in the Hamiltonian (3.1) is included for

later convenience and the angular brackets mean that each pair is only counted once.

A. Mean-field theory

The mean-field or virtual-crystal approximation to the Hamiltonian (3.1) assigns the same value of the magnetization $M = \langle S_i^z \rangle$ to each site so that the self-consistent equation for the magnetization becomes

$$M = SB_S[4\beta Mz(J_1Sp + J_2S(1-p))] , \qquad (3.3)$$

where $B_S[x]$ is the Brillouin function[4] for spin S and z is the number of nearest neighbors. Near the critical point where M is small, we can put $B_S[x] \simeq x(S+1)/3S$,

$$M \simeq 4\frac{S(S+1)}{3}\beta_c Mz(J_1Sp + J_2S(1-p)) \qquad (3.4)$$

and

$$T_c(p) = (1-p)T_c(0) + pT_c(1) , \qquad (3.5)$$

which is just linear extrapolation between $T_c(0)$ and $T_c(1)$. For the rest of this section we shall only be concerned with the case where $S = \frac{1}{2}$ and so we will rewrite the Hamiltonian

$$H = -\sum_{\langle ij \rangle} J_{ij}\sigma_i\sigma_j , \qquad (3.1')$$

where $\sigma_i = \pm 1$ with the same probability distribution of exchanges Eq. (3.2).

B. Annealed model

The phase diagram for this system has been obtained by Thorpe and Beeman[5] for *annealed disorder* in which correlations are introduced so that the joint probability for two bonds $P(J_{ij},J_{kl})$ does not factorize into

$$P(J_{ij},J_{kl}) \neq P(J_{ij})P(J_{kl}) , \qquad (3.6)$$

where $P(J_{ij})$ is given by Eq. (3.2). Thorpe and Beeman[5] showed that these correlations were extremely small when there was no competition between exchange interactions of opposite signs. The expression for the phase boundary [Thorpe and Beeman,[5] Eq. (13)] becomes

$$\frac{p}{\coth(K_c - \beta_c J_1) - \epsilon_c} + \frac{1-p}{\coth(K_c - \beta_c J_2) - \epsilon_c} = 0 ,$$
$$(3.7)$$

where K_c and ϵ_c are the values at the critical point of the interaction parameter βJ and the nearest-neighbor correlation $\langle \sigma_1 \sigma_2 \rangle$ for a non-random system on the same lattice. These parameters are

known exactly in two dimensions. For the square lattice $\epsilon_c = 1/\sqrt{2}$ and $\exp(2K_c) = 1 + \sqrt{2}$ (Onsager[6]).

For small p, the result (3.7) can be expanded to give the initial slope of the phase boundary (putting $J_1 = \lambda J_2$).

$$\frac{1}{T_c}\frac{\partial T_c}{\partial p} = \frac{1}{K_c}[\epsilon_c + \coth K_c(\lambda - 1)]^{-1} . \qquad (3.8)$$

C. Perturbation theory

This result (3.8) is identical with the result that is obtained from perturbation theory in which a single bond J_1 is embedded in a lattice where all the other bonds are J_2. This is shown in detail in Appendix B. The result is not surprising because if a *single* bond is allowed to migrate through the lattice, as in the annealed version of the problem, nothing is changed as all possible positions are equivalent and so the annealing has no effect and introduces no error. From the initial slopes it is easy to show that the phase boundary is always *below* the mean-field result which would be a straight line between the transition temperatures at $p = 0$ and $p = 1$. Thus for bond disorder we have the situation B shown in Fig. 1 for all values of J_1, $J_2 > 0$ and for all lattices. This has been shown to be correct at all concentrations by Falk and Gehring.[7] In Figs. 2 and 3 we show phase diagrams for various values of the ratio $\lambda = J_1/J_2$. The bowing down can clearly be seen in these figures. As $\lambda = J_1/J_2$ increases, the initial slope near $p = 0$ approaches a limiting value which from Eq. (3.8) is given by

$$\frac{1}{T_c}\frac{\partial T_c}{\partial p} \rightarrow \frac{1}{K_c}(\epsilon_c + 1)^{-1} . \qquad (3.9)$$

In fact the initial slope is bounded from both above and below as the coth function in Eq. (3.8) always lies outside ± 1. For the square net this leads to the inequality

$$-7.747 < \frac{1}{T_c}\frac{\partial T_c}{\partial p} < 1.329 . \qquad (3.10)$$

In the *dilute* bond case ($\lambda = 0$) we have

$$\frac{1}{T_c}\frac{\partial T_c}{\partial p} = -1.329 . \qquad (3.11)$$

The corresponding expressions for the honeycomb lattice are

$$-6.597 < \frac{1}{T_c}\frac{\partial T_c}{\partial p} < 0.858 \qquad (3.10')$$

and for the *dilute* case

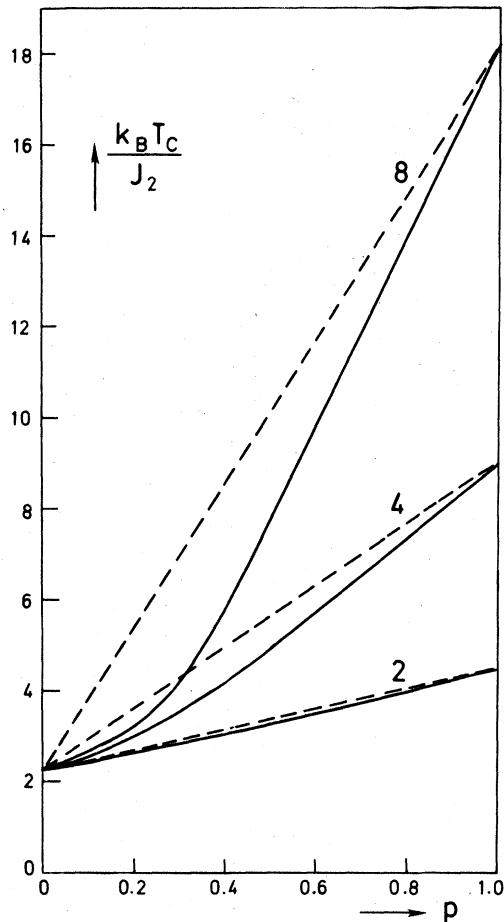$$\frac{1}{T_c}\frac{\partial T_c}{\partial p} = -1.578 . \qquad (3.11')$$

FIG. 2. Phase diagram for the annealed spin-$\frac{1}{2}$ Ising
bond alloy Ref. (5) on a square lattice with exchange in-
teractions J_1 and $J_1 = \lambda J_2$, for various values of $\lambda > 1$. The
dashed lines are for guidance of the eye and p is the concen-
tration of bonds with strength J_1.

As $\lambda = J_1/J_2 \rightarrow 0$, the alloy becomes a dilute bond
ferromagnet and the transition temperature goes to
zero at the percolation concentration p_c which is $\frac{1}{2}$
for the square net.

For the square net with $p = \frac{1}{2}$, Eq. (3.7) can be
rewritten

$$\sinh(2\beta_c J_1) \sinh(2\beta_c J_2) = 1 , \qquad (3.12)$$

which is the expression originally derived by Onsager[6]
for the square net where all the vertical bonds are J_1
and all the horizontal bonds are J_2. It has recently
been shown by Fisch[8] that Eq. (3.12) also holds when
the bonds are arranged randomly. It therefore ap-
pears that our expression (3.7) for the phase boun-
dary of the annealed alloy coincides with the
quenched alloy small p, for small $p' = 1-p$ and for
$p = \frac{1}{2}$, and so can be regarded as an interpolation for-
mula between these known results for the quenched
alloy.

D. Bethe lattice

We note that the phase boundary for the Ising fer-
romagnet on the Bethe lattice (no closed loops) is
given by the very simple expression[9]

$$(z - 1)^{-1} = p \tanh\beta_c J_1 + (1 - p) \tanh\beta_c J_2 , \quad (3.13)$$

which is qualitatively the same as shown in Figs. 2
and 3 as would be expected. Note that the phase
boundaries for the spin-$\frac{1}{2}$ Ising model on the Bethe
lattice are identical for both quenched and annealed
disorder. This is because the high-temperature
behavior is identical due to the spin correlation func-
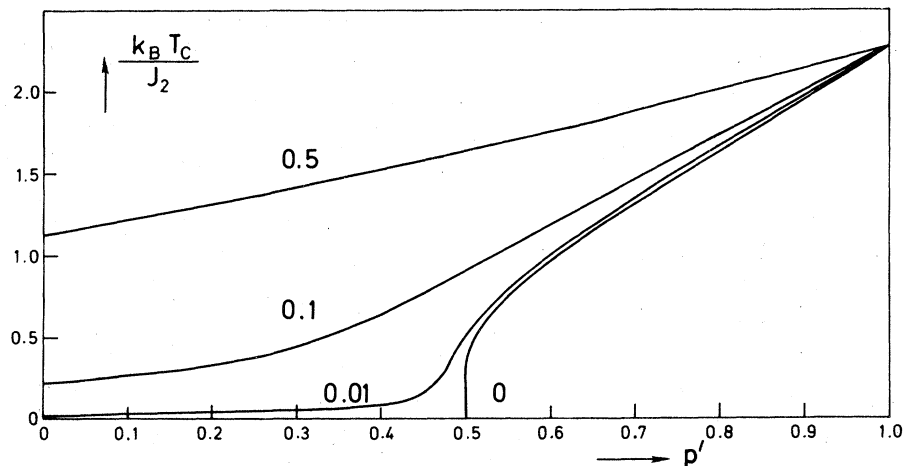tion between any two points behaving as in a linear

FIG. 3. Phase diagram for the annealed spin-$\frac{1}{2}$ Ising bond alloy Ref. (5) on a square net with exchange interactions J_1 and
$J_1 = \lambda J_2$, for various values of λ where $0 \leqslant \lambda < 1$. The percolation limit ($\lambda = 0$, $T_c = 0$) is shown and $p' = 1-p$ is the concentra-
tion of bonds with strength J_2.

chain. The low-temperature phases are rather sensitive to the boundary conditions used.[10]

IV. SITE DISORDER

The site alloy is more complicated than the bond alloy because changing a single site means that all the bonds that terminate on that site are affected and that more than just the nearest-neighbor spin-spin correlation function of the pure system is involved. However the necessary correlation functions can readily be found for lattices with low-coordination numbers, and we examine the honeycomb and square lattices in this section. The Hamiltonian for the system is

$$H = -4 \sum_{\langle ij \rangle} [p_i p_j J_{AA} + p_i (1-p_j) J_{AB} + (1-p_i) p_j J_{BA}$$

$$+ (1-p_j)(1-p_j) J_{BB}] S_i^z S_j^z , \qquad (4.1)$$

where p_i is 1 if site i is occupied by an A-type (with probability p) atom and zero if occupied by a B-type atom (with probability $1-p$).

A. Mean-field theory

The mean-field or virtual-crystal approximation assumes that *all* the A sites have the same magnetization M_A and *all* the B sites have the same magnetization M_B. This leads to a pair of coupled equations involving the three possible exchanges J_{AA}, J_{BB}, and $J_{AB} = J_{BA}$, and the spins S_A and S_B of the two magnetic species

$$M_A = S_A B_{S_A}[4\beta z S_A (J_{AA} p M_A + J_{AB}(1-p) M_B)] ,$$
$$\qquad\qquad (4.2)$$
$$M_B = S_B B_{S_B}[4\beta z S_B (J_{BA} p M_A + J_{BB}(1-p) M_B)] .$$

Near the critical point M_A and M_B are small so that

$$M_A \cong 4\frac{S_A(S_A+1)}{3}\beta_c z [J_{AA} p M_A + J_{AB}(1-p) M_B] ,$$
$$\qquad\qquad (4.3)$$
$$M_B \cong 4\frac{S_B(S_B+1)}{3}\beta_c z [J_{BA} p M_A + J_{BB}(1-p) M_B] .$$

Solving this pair of equations gives

$$k_B T_c = \frac{2z}{3}(S_A(S_A+1) J_{AA} p + S_B(S_B+1) J_{BB}(1-p)$$

$$+ \{[S_A(S_A+1) J_{AA} p + S_B(S_B+1) J_{BB}(1-p)]^2$$

$$+ 4 S_A(S_A+1) S_B(S_B+1) p(1-p)$$

$$\times (J_{AB}^2 - J_{AA} J_{BB})\}^{1/2}) . \quad (4.4)$$

We see that the important quantity in determining the nature of the phase boundary is

$$\Delta = J_{AB}^2 - J_{AA} J_{BB} . \qquad (4.5)$$

If $\Delta = 0$, the phase boundary is a straight line; if
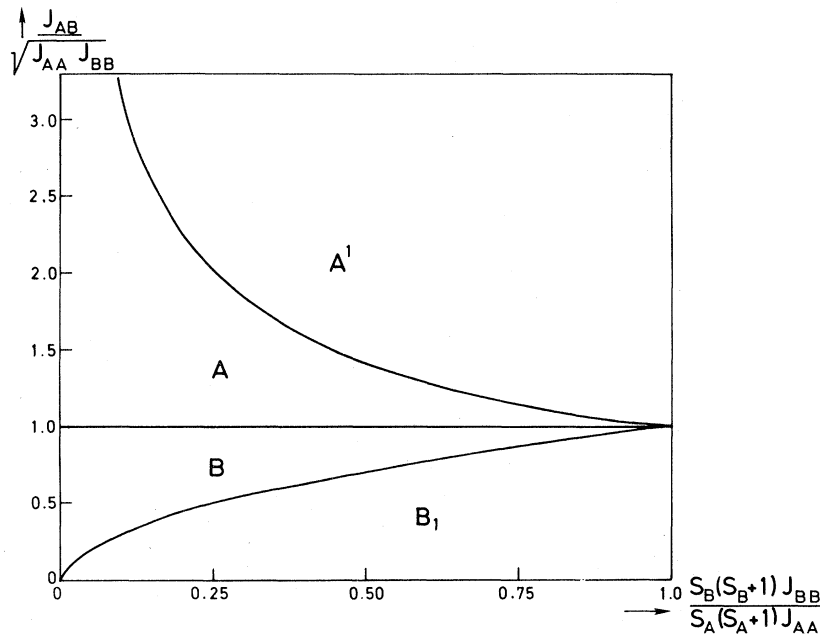

FIG. 4. Possible kinds of phase diagrams (see Fig. 1) that can occur in mean-field theory for an A,B site alloy with spins S_A and S_B and with exchange interactions J_{AA}, J_{BB}, and J_{AB}.

$\Delta > 0$ it bows upwards and if $\Delta < 0$ it bows downwards. It should be noted that Δ is very close to zero for many transition-metal compounds.[1] We will discuss the relevance of these results to real systems at the end of the paper. Near the $p = 0$ the phase boundary has a negative slope if

$$S_A(S_A + 1)J_{AA} > [S_A(S_A + 1)S_B(S_B + 1)]^{1/2}J_{AB} , \quad (4.6)$$

with a similar relation near $p = 1$. These results can be conveniently presented in graphical form as shown in Fig. 4. We see that only four kinds of phase diagrams are permitted from the nine possible ones sketched in Fig. 1. The mean-field result is very useful in providing a frame of reference in which to discuss subsequent results. Note that by absorbing the spins into the exchange parameters so that

$$j_{AA} = S_A(S_A + 1)J_{AA} ,$$

$$j_{BB} = S_B(S_B + 1)J_{BB} , \quad (4.7)$$

$$j_{AB} = [S_A(S_A + 1)S_B(S_B + 1)]^{1/2}J_{AB} ,$$

the mean-field results become independent of the spin magnitude and depend only on j_{AA}, j_{BB}, and j_{AB}. These considerations have been used in choosing suitable axes in Fig. 4.

B. Perturbation theory—spin $\frac{1}{2}$

We examine the Hamiltonian (4.1) for spin $\frac{1}{2}$ where $S_i^z = \frac{1}{2}\sigma_i$.

$$H = -\sum_{\langle ij \rangle} [p_i p_j J_{AA} + p_i(1-p_j)J_{AB} + (1-p_i)p_j J_{BA}$$

$$+ (1-p_i)(1-p_j)J_{BB}]\sigma_i\sigma_j . \quad (4.1')$$

A single impurity site is introduced into an otherwise perfect lattice as shown in Fig. 5 for the honeycomb lattice and Fig. 6 for the square lattice. The
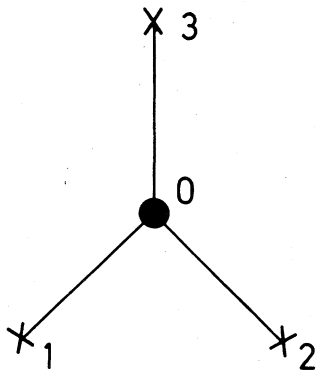

FIG. 5. Single impurity in a honeycomb lattice. The impurity is labelled 0 and its three nearest neighbors 1, 2, and 3.
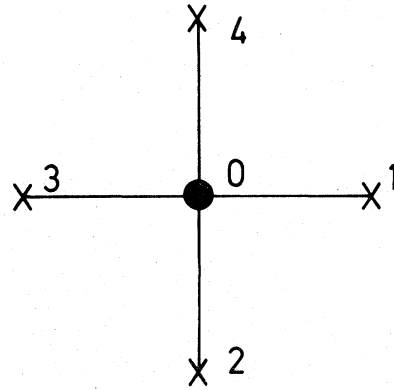

FIG. 6. Single impurity in a square lattice. The impurity is labelled 0 and its four nearest neighbors 1, 2, 3, and 4.

host is characterized by an exchange J and the impurity has z nearest neighbors to which it is connected with an exchange λJ. This corresponds to putting $J_{BB} = J$, $J_{AB} = \lambda J$, and J_{AA} which is irrelevant can be set equal to zero, for small p in the Hamiltonian (4.1'). For the honeycomb lattice, the initial slope of the phase diagram can be expressed entirely in terms of the nearest-neighbor correlation function $\langle \sigma_0 \sigma_1 \rangle$ as shown in Appendix C. This does not seem to have been noted in the literature previously. The initial slope [Eq. (C7)] is given by

$$\frac{1}{T_c}\frac{\partial T_c}{\partial p} = \frac{2}{\sqrt{3}K_c}[1 - 2\operatorname{sech}(2K_c\lambda)] , \quad (4.8)$$

where $\cosh(2K_c) = 2$.[11]

The square net is more complicated, but the necessary correlation functions have been studied previously.[12] The result for the initial slope [Eq. (D6)] is derived in Appendix D. The parameter λ takes on the values J_{AB}/J_{AA} or J_{AB}/J_{BB} depending on which end of the phase boundary we are considering. The slope can then be examined to see in which of the three regions 1, 2, 3 in Fig. 1 it occurs.

In Figs. 7 and 8 we show the various kinds of phase diagrams that can occur for the honeycomb and square lattices respectively as the exchange interactions J_{AA}, J_{BB}, and J_{AB} are varied. There is a much greater variety of possible behavior in the site problem as contrasted with the bond problem. This is because an extra parameter J_{AB} is involved in the disorder. Comparing Figs. 7 and 8 we see that they are quite similar. Two kinds of phase diagram S and S' can occur that do not exist in mean-field theory (see Fig. 4). The region of parameter space where B occurs is considerably expanded while the A and A' regions are shrunk. Indeed it can be shown by examining the expressions for the initial slope $(1/T_C)(\partial T_c/\partial p)$ that *the phase boundary in mean-field theory for the $S = \frac{1}{2}$ Ising model always lies*
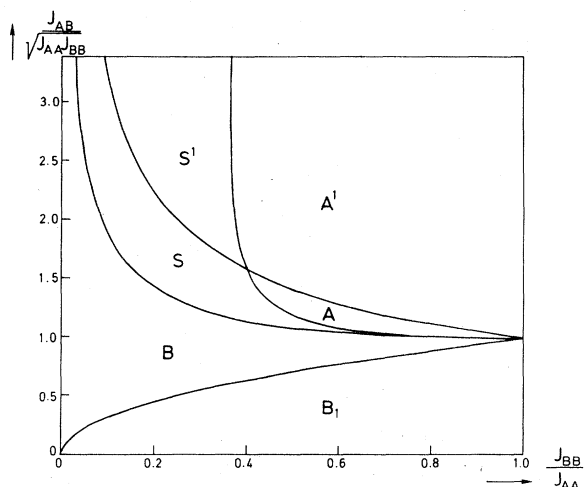
FIG. 7. Spin-$\frac{1}{2}$ site alloy on the honeycomb lattice. The various kinds of phase diagrams that can occur are shown for different parts of parameter space (see Fig. 1 for an explanation of the symbols).

above the true phase boundary near p = 0 and p = 1. This result is not surprising as mean-field theory always overestimates T_c in pure systems. Even when this overestimation is taken out by dividing by T_c and examining $(1/T_c)(\partial T_c/\partial p)$, the result is still too high because the fluctuations due to the randomness are suppressed. It is probable that the *complete* phase diagram is below mean-field theory (with the temperature axis rescaled so that the transition temperatures at p = 0 and p = 1 are the same) but of course this

cannot be shown using the perturbation theory described in this paper.

C. Bethe lattice

Unfortunately there is no approximate theory for real lattices for the site disordered alloy which provides a reasonable interpolation for general concentration p and is correct in the two limits $p \rightarrow 0$ and $p \rightarrow 1$. In order to illustrate the results for the site alloy we have examined the phase boundary for the Bethe lattice, which is known exactly[9] and given by

$$1 = (z-1)[p \tanh(\beta_c J_{AA}) + (1-p) \tanh(\beta_c J_{BB})]$$

$$- \{(z-1)^2 p(1-p)[\tanh(\beta_c J_{AA}) \tanh(\beta_c J_{BB})$$

$$- \tanh^2(\beta_c J_{AB})]\} . \quad (4.9)$$

Figure 9 shows the various kinds of phase diagrams that can occur in different regions of exchange parameter space, and Fig. 10 shows the complete phase diagrams for selected values of J_{AA}, J_{BB}, and J_{AB}. It can be seen that these are always the simplest possible that are compatible with the initial slopes and *do not have any extra wiggles*. As the results for the Bethe lattice in Fig. 9 are very similar qualitatively to those for the honeycomb and square lattices, we expect that this is generally true.
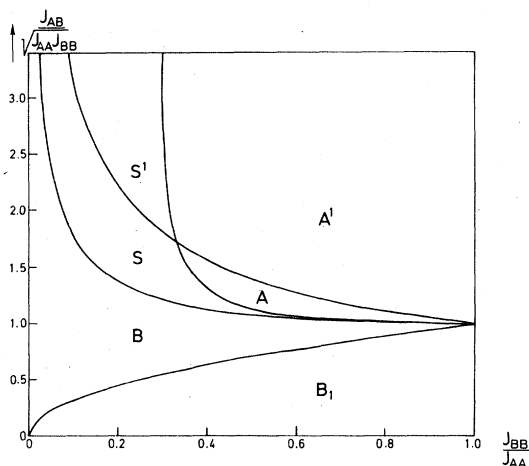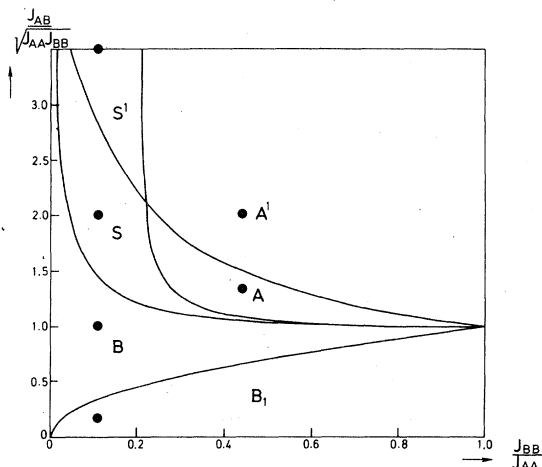

FIG. 8. Spin-$\frac{1}{2}$ site alloy on the square lattice. The various kinds of phase diagrams that can occur are shown for different parts of parameter space (see Fig. 1 for an explanation of the symbols).

FIG. 9. Spin-$\frac{1}{2}$ site alloy on a z = 3 Bethe lattice. The various kinds of phase diagrams that can occur are shown for different parts of parameter space (see Fig. 1 for an explanation of the symbols). The solid circles mark points in the parameter space for which the complete phase boundary is shown in Fig. 10.
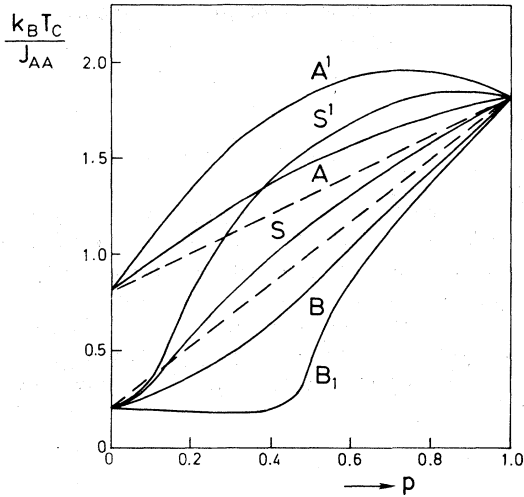
FIG. 10. Complete phase boundary for the spin-$\frac{1}{2}$ site alloy on a $z = 3$ Bethe lattice for the special points shown in Fig. 9. The ratios of $J_{AA}:J_{AB}:J_{BB}$ for the points considered are: A^1; 18:24:8, A; 18:16:8, S; 18:12:2, S^1; 18:21:2, B; 18:6:2, B_1; 18:1:2. The dashed lines are for guidance of the eye only.

D. Perturbation theory $S > \frac{1}{2}$

This same kind of perturbation theory can be extended to the case when the impurity spin S is greater than $\frac{1}{2}$ as first noted by Watson[13] for $S = 1$. Of course the corresponding perturbation theory at the other end of the phase boundary, where there is a spin $\frac{1}{2}$ impurity in a spin $S > \frac{1}{2}$ host, cannot be done as the pure system solution is not known. We are therefore restricted to discussing what happens at one end of the phase diagram only.

The Hamiltonian for the pure spin-$\frac{1}{2}$ system is given by

$$H_0 = -J \sum_{\langle ij \rangle} \sigma_i \sigma_j , \qquad (4.10)$$

where the summation is over nearest neighbors only and $\sigma_i = \pm 1$. A single impurity spin at a site labelled 0 interacts via

$$H_{\text{int}} = -2\alpha J \sum_\delta S_0 \sigma_\delta , \qquad (4.11)$$

where δ goes over the z nearest neighbors of the impurity site and we include the factor 2 so that when the impurity spin $S = \frac{1}{2}$, we recover the solution given in Sec. IV B with $\alpha = \lambda$.

The partition function for the system with the single-site impurity may be written

$$z''(S) = \text{Tr}[e^{-\beta H_{00}} \exp(2\beta \alpha J S_0 \sum_\delta \sigma_\delta)] , \qquad (4.12)$$

where H_{00} is the same as H_0 given in Eq. (4.10) but with all the terms involving σ_0 omitted. The trace in Eq. (4.12) goes over all σ except σ_0, and over S_0. Doing the trace over S_0, the terms can be paired together $\pm S$, $\pm (S-1) \ldots \pm \frac{1}{2}$ or 0, depending on whether $2S$ is even or odd. We find that

$$z''(S) = z'(2\alpha S) + z'(2\alpha(S-1)) + \cdots$$
$$+ \begin{cases} z'(\alpha), & 2S \text{ even,} \\ \frac{1}{2} z'(0), & 2S \text{ odd,} \end{cases} \qquad (4.13)$$

where $z'(\lambda)$ is the partition function for a spin-$\frac{1}{2}$ impurity given in Appendices C and D for the honeycomb and square lattices. The energy can be calculated from the partition function and using similar arguments to those used for spin $\frac{1}{2}$ we can calculate the initial slope.

For the honeycomb lattice, we find that expanding T_c about $p = 0$,

$$\frac{1}{T_c} \frac{\partial T_c}{\partial p} = \frac{2}{\sqrt{3}K_c} \left[\frac{f_3(\alpha) - 3f_1(\alpha)}{f_3(\alpha) + f_1(\alpha)} \right] , \qquad (4.14)$$

while for the square lattice

$$\frac{1}{T_c} \frac{\partial T_c}{\partial p} = \frac{1}{\sqrt{2}K_c}$$
$$\times \left[\frac{\pi[\sqrt{2}f_2(\alpha) - 2] + g(\alpha)}{\pi[\sqrt{2}f_2(\alpha) - 1] + (1 - 1/\pi)g(\alpha)} \right] , \qquad (4.15)$$

where

$$f_R(\alpha) = \frac{\sinh[(2S+1)K_c\alpha R]}{(2S+1)\sinh[K_c\alpha R]} \qquad (4.16)$$

and

$$g(\alpha) = f_4(\alpha) - 4\sqrt{2}f_2(\alpha) + 5 . \qquad (4.17)$$

Putting $S = \frac{1}{2}$ in these expressions we recover the results found previously of course. As we found for bond disorder, not all values of the initial slope are possible. Letting $\alpha^2 \to 0$ and ∞ respectively we find the following inequality on the square net:

$$-1.565 < \frac{1}{T_c} \frac{\partial T_c}{\partial p} < 2.354 . \qquad (4.18)$$

For the special case of the dilute site problem

$$\frac{1}{T_c} \frac{\partial T_c}{\partial p} = -1.565 . \qquad (4.19)$$

Similarly for the honeycomb lattice we have

$$-1.754 < \frac{1}{T_c} \frac{\partial T_c}{\partial p} < 1.754 \qquad (4.20)$$

and for the dilute site problem on the honeycomb lattice

$$\frac{1}{T_c}\frac{\partial T_c}{\partial p} = -1.754 \ . \qquad (4.21)$$

Both the expressions (4.14) and (4.15) are even functions of α. That is it makes no difference whether the impurity is coupled ferromagnetically or antiferromagnetically and this leads to the upper bound in the inequalities above. This result is perhaps a little surprising. However it is clear that the energy does not depend on the sign of α and so T_c is also unaffected by the sign of α. The lower limit in the inequalities above are always given by the dilute problem ($\alpha = 0$) which therefore represents an extremum. This situation is sketched in Fig. 11. This behavior is very different from the bond alloy discussed in Sec. III, where antiferromagnetic bonds depress T_c *very much more* than would happen for bond dilution as can be seen by the very large low limits in Eqs. (3.10) and (3.10'). It should be emphasized that apart from this comment and the similar one in Sec. III, all the work in this paper is concerned with the case where all the interactions have the same sign.

We examine the conditions that lead to a *zero initial slope*. If we define

$$r(S) = [4S(S+1)\alpha^2/3]^{1/2} \qquad (4.22)$$

then the mean-field theory described at the beginning of this section predicts that $r(S) = 1$ for all spin values for all lattices. We find from Eq. (4.14) that $r(S) = 1, 0.923, 0.912,$ and 0.905 for $S = \frac{11}{2}, \frac{3}{2}, \frac{5}{2}$, and ∞ for the honeycomb lattice; and $1, 0.935, 0.926,$ and 0.919 for the square lattice.
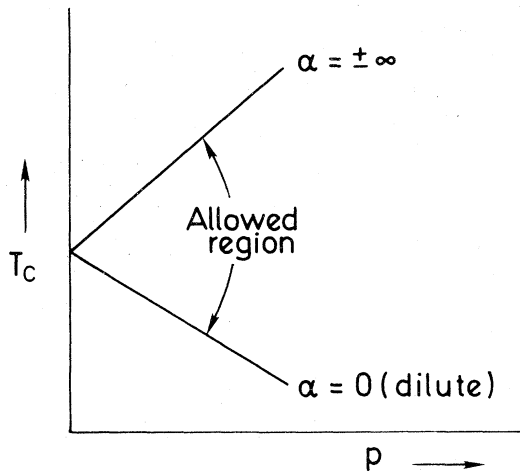

FIG. 11. Sketch of the allowed regions for the initial slope for the site alloy where the host has spin $\frac{1}{2}$ but the impurity has an arbitrary spin and an arbitrary exchange coupling to the host.

The classical spin limit can be found by letting $S \to \infty$, $\alpha \to 0$ so that $\alpha S = C$ is finite and

$$f_R(\alpha) \to \frac{\sinh(2CK_cR)}{2CK_cR} \ . \qquad (4.23)$$

The result in this limit can also be found more directly as the trace over S_0 in Eq. (4.12) becomes an integral over the solid angle

$$\mathrm{Tr}_{S_0} \to \frac{1}{4\pi} \int \ldots d\Omega_{S_0} \qquad (4.24)$$

that can easily be done.

For $S > \frac{1}{2}$, $\partial(\ln T_c)/\partial p$ can be either greater than or less than the mean-field result depending on the value of α. It is rather difficult to discuss the character of the complete phase boundary in this case as the result for $p = 1$, when all the sites have spin S, is not known exactly. Also a different temperature rescaling would be needed for $p = 0$ and $p = 1$ to make the mean-field results coincide with the exact results.

V. CONCLUSIONS

We have shown that perturbation theory can be useful both in classifying and in understanding the kinds of phase diagrams that can occur in systems where all the interactions have the same sign. We have found that mean-field behavior generally overestimates T_c in the mixed region for spin $\frac{1}{2}$ even when normalized so as to coincide with the exact results at $p = 0$ and $p = 1$. We have also shown that the initial slope of the phase boundary is not very sensitive to the spin S if properly scaled variables are used.

We have shown that not all values of the initial slope are allowed but that they must fall within a rather broad range. In particular in the site alloy, the slope for the dilute case represents an extremum as the system is not sensitive to the difference between ferromagnetically and antiferromagnetically coupled impurities. It is therefore not possible for T_c to decrease faster than it does for vacancies.

There is surprisingly little experimental data published on the critical temperatures of A-B alloys and that which there is involves systems with more complicated interactions than just Ising. Indeed many of the transition-metal compounds studied in Ref. 1 involve Heisenberg interactions. However it is probable that most of our qualitative conclusions about the nature of the phase boundary do not depend on the precise nature of the interactions. Most of the insulating magnetic alloys studied are antiferromagnetic rather than ferromagnet. However as long as there is no competition brought about by odd membered rings, such as the triangles in the fcc lattice, our general conclusions should apply. For example in $\mathrm{Rb_2Mn}_p\mathrm{Ni}_{1-p}\mathrm{F_4}$ it is found[1] that $T_c = 38.4,\ 63.7,$

and 91 K for $p = 0$, 0.5, and 1. It is known that $J_{AB} = (J_{AA}J_{BB})^{1/2}$ in this system[14] so that mean-field theory predicts a linear phase boundary. In fact it bows downward because $63.7 < \frac{1}{2}(38.4 + 91)$. This is consistent with the calculations described in Sec. IV.

ACKNOWLEDGMENT

APPENDIX A

In order to derive an expression for the change in the transition temperature from the energy, a number of very reasonable assumptions have to be made. We will give the argument for a temperature T just above T_c but it can be made equally well for T just below T_c. If we write the specific heat C as

$$C = A(p)[T - T_c(p)]^{-\alpha(p)} \tag{A1}$$

then

$$\frac{1}{C}\frac{\partial C}{\partial p} = \frac{1}{A}\frac{\partial A}{\partial p} - \frac{\partial \alpha}{\partial p}\ln(T - T_c) + \frac{\alpha}{(T - T_c)}\frac{\partial T_c}{\partial p} . \tag{A2}$$

It is clear that if $A(p)$, $T_c(p)$, and $\alpha(p)$ are reasonably behaved for small p, then the last term in Eq. (A2) is dominant. The energy E can be written

$$E = \text{const} + \frac{A}{-\alpha + 1}(T - T_c)^{-\alpha + 1} \tag{A3}$$

and therefore

$$\frac{\partial E}{\partial p} = -A(T - T_c)^{-\alpha}\frac{\partial T_c}{\partial p}$$

$$= -C\frac{\partial T_c}{\partial p} . \tag{A4}$$

This expression allows $\partial T_c/\partial p$ to be found. This equation must be interpreted as involving only the most divergent parts, i.e., C and $\partial E/\partial p$ are divergent while $\partial T_c/\partial p$ is finite. The divergent parts cancel out to give the desired result for $\partial T_c/\partial p$ for any particular system. It must be emphasized that Eq. (A4) only applies if the specific heat of the pure system is infinite at the critical point. It is valid if the specific heat diverges logarithmically as in the two-dimensional Ising model.

For small p, the energy E can often be written

$$E = E_0 - Np\frac{\partial}{\partial \beta}\ln(a + b\epsilon) , \tag{A5}$$

where E_0 is the energy of the pure system, N is the number of bonds, a, b are functions of T, and ϵ is the nearest-neighbor correlation function $\langle \sigma_1 \sigma_2 \rangle$.

Noting that C can be written

$$C = \frac{N\beta J}{T}\frac{\partial \epsilon}{\partial \beta} \tag{A6}$$

we see from Eqs. (A4), (A5), and (A6) that

$$\frac{1}{T_c}\frac{\partial T_c}{\partial p} = \frac{1}{K_c}\frac{1}{\epsilon_c + a/b} , \tag{A7}$$

where ϵ_c and $K_c = \beta_c J$ are the values at the critical point. This expression is exact given the reasonable assumptions made above. It is probable that these arguments can be made rigorous; great care must be taken however with the $p \to 0$ and $T \to T_c$ limits. Similar arguments have been used by Osawa and Sawada.[15] When the energy cannot be written entirely in terms of ϵ as in Eq. (A5), then the temperature can be considered $T(\epsilon)$ and an expression obtained for $\partial(\ln T_c)/\partial p$ as is shown in Appendix D for the square net. Identical results for $\partial(\ln T_c)/\partial p$ can be obtained by considering the functional form of the magnetization rather than the specific heat as in Eq. (A1). This is slightly more general as one only has to assume that the magnetization goes to zero at the critical point rather than the specific heat diverging. The result Eq. (A4) therefore applies to Ising Bethe lattices where the specific heat is finite at the critical point when approached from the high-temperature side. It would also apply to the Heisenberg model in three dimensions, although not enough is known about this model for it to be useful.

APPENDIX B

For the case of bond impurities in an Ising lattice [see Eqs. (3.1') and (3.2)], it is possible to find the behavior of the phase boundary for small p or small $q = 1 - p$ using thermodynamic perturbation theory.[13] The partition function z' for a system with a single defect bond $J' = \lambda J$, embedded in an otherwise perfect system with exchanges J, may be written

$$z'(\lambda) = z_0\langle e^{\beta(\lambda - 1)J\sigma_1\sigma_2}\rangle_0 , \tag{B1}$$

where z_0 is the partition function for the pure system without a defect (i.e., λJ replaced by J) and the thermal average is to be taken in the pure system. The spins σ_1, σ_2 are at the ends of the defect bond. With a little manipulation Eq. (B1) may be rewritten

$$z'(\lambda) = z_0[\cosh\beta(\lambda - 1)J + \langle \sigma_1\sigma_2 \rangle_0 \sinh\beta(\lambda - 1)J] . \tag{B2}$$

The energy can be obtained from the partition function in the usual way ($E = -\partial \ln z'/\partial \beta$) to give

$$E = E_0 - 2\frac{\partial}{\partial \beta}\ln[\cosh\beta(\lambda - 1)J + \epsilon\sinh\beta(\lambda - 1)J] , \tag{B3}$$

where $\epsilon = \langle \sigma_1 \sigma_2 \rangle_0$ and E_0 is the energy of the pure system. If there are a small number Np defect bonds that are so widely separated that they are essentially noninteracting, then a factor Np can be inserted before the second term in Eq. (B3), to give an expression of the general form Eq. (A5). The initial slope of the phase boundary is therefore given by Eq. (A7) and is

$$\frac{1}{T_c}\frac{\partial T_c}{\partial p} = \frac{1}{K_c}[\epsilon_c + \coth K_c(\lambda - 1)]^{-1} . \tag{B4}$$

This expression is the same as derived from the annealed bond model given in Eq. (3.8).

APPENDIX C

The honeycomb lattice is actually easier to treat in perturbation theory than the square lattice that has been more extensively discussed in the literature.[12] The impurity site is labelled zero as shown in Fig. 5 and its three neighbors are labelled 1, 2, and 3. The three bonds from the impurity site have exchanges λJ associated with them while all the other bonds in the lattice are J. The partition function z' for this situation may be written

$$z'(\lambda) = z_0 \cosh^3[\beta J(\lambda - 1)]$$
$$\times \langle (1 + t\sigma_0\sigma_1)(1 + t\sigma_0\sigma_2)(1 + t\sigma_0\sigma_3) \rangle_0 ,$$
$$\tag{C1}$$

where z_0 is the partition function for the pure system and

$$t = \tanh[\beta J(\lambda - 1)] . \tag{C2}$$

The correlation function that appears in Eq. (C1) may be multiplied out to give

$$1 + 3t\langle \sigma_0\sigma_1 \rangle_0 + 3t^2\langle \sigma_1\sigma_2 \rangle_0 + t^3\langle \sigma_0\sigma_1\sigma_2\sigma_3 \rangle_0 ,$$
$$\tag{C3}$$

where we have used the equivalence of the three sites to simplify the expression. The expressions in Eq. (C3) can all be expressed in terms of $\epsilon = \langle \sigma_0\sigma_1 \rangle_0$. If O is any operator that does *not* involve σ, then by doing a partial trace over σ_0 it is easy to show that

$$\langle \sigma_0 O \rangle_0 = A \langle (\sigma_1 + \sigma_2 + \sigma_3) O \rangle_0 + B \langle \sigma_1\sigma_2\sigma_3 O \rangle_0 ,$$
$$\tag{C4}$$

where

$$A = \frac{1}{4}[\tanh 3K + \tanh K] ,$$
$$B = \frac{1}{4}[\tanh 3K - 3\tanh K] , \tag{C5}$$

and $K = \beta J$. Putting $O = \sigma_1$ and then $O = \sigma_1\sigma_2\sigma_3$,

respectively, we find that

$$\langle \sigma_0\sigma_1 \rangle_0 = A[1 + 2\langle \sigma_1\sigma_2 \rangle_0] + B\langle \sigma_1\sigma_2 \rangle_0 \tag{C6}$$

and

$$\langle \sigma_0\sigma_1\sigma_2\sigma_3 \rangle = 3A\langle \sigma_1\sigma_2 \rangle_0 + B .$$

Thus the expression (C3) has the form $a + b\epsilon$ and we can use the result of Appendix A (an extra factor $\frac{2}{3}$ must be inserted because we are dealing with site impurities rather than bond impurities). At the critical point $\epsilon_c = 4\sqrt{3}/9$ and $\exp(2K_c) = 2 + \sqrt{3}$ and so we have, expanding about $T_c(0)$,

$$\frac{1}{T_c}\frac{\partial T_c}{\partial p} = \frac{2}{\sqrt{3}K_c}[1 - 2\operatorname{sech}(2K_c\lambda)] . \tag{C7}$$

APPENDIX D

A single spin impurity in an otherwise perfect square net has been treated extensively in the literature[12] and we will only sketch the result. The impurity is labelled 0 as shown in Fig. 6 and its four neighbors labelled 1, 2, 3, and 4. The four bonds from the impurity site have exchanges λJ associated with them while all the other bonds in the lattice are J. Using similar notation to that in Appendix C, the partition function z' may be written

$$z'(\lambda) = z_0 \cosh^4[\beta J(\lambda - 1)]\langle \prod_{i=1}^{4}(1 + t\sigma_0\sigma_i) \rangle_0 . \tag{D1}$$

Expanding the brackets leads to both two- and four-spin correlation functions. The four-spin correlation functions can be expressed in terms of two-spin correlation functions using arguments similar to those in Appendix C for the honeycomb lattice.[12]

$$\langle \sigma_0 O \rangle_0 = A\langle (\sigma_1 + \sigma_2 + \sigma_3 + \sigma_4) O \rangle_0$$
$$+ B[\langle \sigma_1\sigma_2\sigma_3 O \rangle_0 + \langle \sigma_2\sigma_3\sigma_4 O \rangle_0$$
$$+ \langle \sigma_3\sigma_4\sigma_1 O \rangle_0 + \langle \sigma_4\sigma_1\sigma_2 O \rangle_0] , \tag{D2}$$

where O is any operator *not* involving σ_0 and

$$A = \frac{1}{8}[\tanh 4K + 2\tanh 2K] ,$$
$$B = \frac{1}{8}[\tanh 4K - 2\tanh 2K] . \tag{D3}$$

Putting $O = \sigma_1$ and then $O = \sigma_1\sigma_2\sigma_3$ respectively, we find that

$$\langle \sigma_0\sigma_1 \rangle_0 = A[1 + 2\langle \sigma_1\sigma_2 \rangle_0 + \langle \sigma_1\sigma_3 \rangle_0]$$
$$+ B[2\langle \sigma_1\sigma_2 \rangle_0 + \langle \sigma_1\sigma_3 \rangle_0$$
$$+ \langle \sigma_1\sigma_2\sigma_3\sigma_4 \rangle_0] \tag{D4}$$

and

$$\langle \sigma_0 \sigma_1 \sigma_2 \sigma_3 \rangle_0 = A \left[2 \langle \sigma_1 \sigma_2 \rangle_0 + \langle \sigma_1 \sigma_3 \rangle_0 + \langle \sigma_1 \sigma_2 \sigma_3 \sigma_4 \rangle_0 \right]$$
$$+ B \left[1 + 2 \langle \sigma_1 \sigma_2 \rangle_0 + \langle \sigma_1 \sigma_3 \rangle_0 \right] . \quad (D5)$$

These expressions are rather more complicated than those for the honeycomb lattice and the result for z' cannot be expressed as a function only of $\epsilon = \langle \sigma_1 \sigma_2 \rangle_0$. However we can use Eq. (A4) if we note that near the critical point,[12]

$$\frac{\pi}{4(2)^{1/2}} \frac{\partial}{\partial T} \langle \sigma_1 \sigma_3 \rangle = \frac{1}{(2)^{1/2}} \frac{\partial}{\partial T} \langle \sigma_1 \sigma_2 \rangle = \frac{\partial}{\partial T} \langle \sigma_0 \sigma_1 \rangle$$

$$= \frac{4J}{\pi k_B T_c^2} \ln \left| 1 - \frac{T}{T_c} \right| .$$

The divergent logarithmic terms cancel on both sides

of the equation and we have the result

$$\frac{1}{T_c} \frac{\partial T_c}{\partial p} = \frac{1}{\sqrt{2} K_c}$$

$$\times \left(\frac{1}{1 - 1/\pi + [\sqrt{2} \cosh(2K_c \lambda) - 2]^{-1}} \right) ,$$

$$(D6)$$

where we have expanded about $T_c(0)$. For the case of a vacancy ($\lambda = 0$) we find that

$$\frac{1}{T_c} \frac{\partial T_c}{\partial p} = -\frac{1}{K_c} \left[1 + \frac{\sqrt{2}}{\pi} \right]^{-1} = -1.565 \quad (D7)$$

a result previously found by placing the vacancies on a superlattice of variable size,[16] and taking the dilute limit.

---

[1] See for example J. M. Baker, J. A. J. Lourens, and R. W. H. Stevenson, Proc. Phys. Soc. 77, 1038 (1961); V. Jaccarino, Phys. Rev. 178, 804 (1968); R. J. Birgeneau, L. R. Walker, H. K. Guggenheim, J. Als-Nielson, and G. Shirane, J. Phys. C 8, L328 (1975); and G. K. Wertheim, H. J. Guggenheim, M. Butler, and V. Jaccarino, Phys. Rev. 178, 804 (1968).

[2] B. M. McCoy and T. T. Wu, Phys. Rev. 176, 631 (1968).

[3] K. Adachi, K. Sato, M. Matsuura, and M. Ohashi, J. Phys. Soc. Jpn. 29, 323 (1970).

[4] See for example C. Kittel, Introduction to Solid State Physics (Wiley, New York, 1953), p. 216.

[5] M. F. Thorpe and D. Beeman, Phys. Rev. B 14, 188 (1976).

[6] L. Onsager, Phys. Rev. 65, 117 (1944).

[7] H. Falk and G. A. Gehring, J. Phys. C 8, L298 (1975).

[8] R. Fisch, J. Stat. Phys. 18, 111 (1978).

[9] S. Katsura, Can. J. Phys. 52, 120 (1974).

[10] See for example T. P. Eggarter, Phys. Rev. B 9, 2989 (1974); and S. Katsura and M. Takizawa, Prog. Theor. Phys. 51, 82 (1974).

[11] See for example L. Syozi, in Phase Transitions and Critical Phenomena, edited by C. Domb and M. S. Green (Academic, New York, 1972), Vol. 1, p. 269.

[12] M. E. Fisher, Phys. Rev. 113, 969 (1959); J. Math. Phys. 4, 124 (1963); F. H. Stillinger, Phys. Rev. 131, 2027 (1963); and J. Stephenson, J. Math. Phys. 7, 1123 (1966).

[13] P. G. Watson, Proc. Phys. Soc. C 1, 575 (1968).

[14] M. F. Thorpe and R. Alben, J. Phys. C 1, 2555 (1976).

[15] T. Osawa and K. Sawada, Prog. Theor. Phys. 49, 83 (1973).

[16] H. Au-Yang, M. E. Fisher and A. E. Ferdinard, Phys. Rev. B 13, 1238 (1976).